Biochemical and Biophysical Research Communications 447 (2014) 334–340

Contents lists available at ScienceDirect

Biochemical and Biophysical Research Communications

journal homepage: www.elsevier.com/locate/ybbrc

Mitochondrial impairment observed in fibroblasts from South African Parkinson's disease patients with *parkin* mutations

Celia van der Merwe [a,*], Ben Loos [b], Chrisna Swart [a], Craig Kinnear [a,c], Franclo Henning [d], Lize van der Merwe [a,e], Komala Pillay [f], Nolan Muller [g], Dan Zaharie [h], Lize Engelbrecht [i], Jonathan Carr [d], Soraya Bardien [a]

[a] Division of Molecular Biology and Human Genetics, Faculty of Medicine and Health Sciences, Stellenbosch University, Cape Town, South Africa
[b] Department of Physiological Sciences, Faculty of Science, Stellenbosch University, Stellenbosch, South Africa
[c] MRC Centre for Molecular and Cellular Biology and the DST/NRF Centre of Excellence for Biomedical TB Research, Stellenbosch University, Cape Town, South Africa
[d] Division of Neurology, Faculty of Medicine and Health Sciences, Stellenbosch University, Cape Town, South Africa
[e] Department of Statistics, University of the Western Cape, Cape Town, South Africa
[f] National Health Laboratory Services (NHLS) Histopathology Laboratory, Red Cross Children's Hospital, Cape Town, South Africa
[g] Division of Anatomical Pathology, Faculty of Medicine and Health Sciences, Stellenbosch University, Cape Town, South Africa
[h] Neuropathology Unit, Division of Anatomical Pathology, Faculty of Medicine and Health Sciences, Stellenbosch University, Cape Town, South Africa
[i] Cell Imaging Unit, Central Analytical Facility, Stellenbosch University, Cape Town, South Africa

ARTICLE INFO

Article history:
Received 26 March 2014
Available online 8 April 2014

Keywords:
Parkinson's disease
Parkin mutations
Mitochondrial dysfunction
Fibroblasts
Muscle

ABSTRACT

Parkinson's disease (PD), defined as a neurodegenerative disorder, is characterized by the loss of dopaminergic neurons in the substantia nigra in the midbrain. Loss-of-function mutations in the *parkin* gene are a major cause of autosomal recessive, early-onset PD. Parkin has been implicated in the maintenance of healthy mitochondria, although previous studies show conflicting findings regarding mitochondrial abnormalities in fibroblasts from patients harboring *parkin*-null mutations. The aim of the present study was to determine whether South African PD patients with *parkin* mutations exhibit evidence for mitochondrial dysfunction. Fibroblasts were cultured from skin biopsies obtained from three patients with homozygous *parkin*-null mutations, two heterozygous mutation carriers and two wild-type controls. Muscle biopsies were obtained from two of the patients. The muscle fibers showed subtle abnormalities such as slightly swollen mitochondria in focal areas of the fibers and some folding of the sarcolemma. Although no differences in the degree of mitochondrial network branching were found in the fibroblasts, ultrastructural abnormalities were observed including the presence of electron-dense vacuoles. Moreover, decreased ATP levels which are consistent with mitochondrial dysfunction were observed in the patients' fibroblasts compared to controls. Remarkably, these defects did not manifest in one patient, which may be due to possible compensatory mechanisms. These results suggest that *parkin*-null patients exhibit features of mitochondrial dysfunction. Involvement of mitochondria as a key role player in PD pathogenesis will have important implications for the design of new and more effective therapies.

1. Introduction

Parkinson's disease (PD) is a common neurodegenerative disorder with global incidence rates of 1–2% in individuals over the age of 65 and 4% over the age of 80 years [1]. Pathologically, PD is defined as the progressive loss of the dopaminergic neurons in the substantia nigra pars compacta in the midbrain and clinical motor symptoms include bradykinesia, postural instability, rigidity and resting tremor. Although PD has been associated with various environmental factors, a number of genes have been found to cause familial PD, with both autosomal dominant and autosomal recessive patterns [2]. To date, the genes involved in autosomal dominant forms of PD include *SNCA*, *LRRK2*, *EIF4G1* and *VPS35*, and those that are implicated in autosomal recessive PD, which result in a loss-of-function, include *parkin*, *PINK1*, *DJ-1* and *ATP13A2* [3].

Parkin mutations are the predominant cause of autosomal recessive PD, and are involved in the early-onset form of the disorder in which individuals typically under the age of 50 are affected

* Corresponding author. Address: Division of Molecular Biology and Human Genetics, Faculty of Medicine and Health Sciences, Stellenbosch University, PO Box 19063, Tygerberg, 750, Cape Town, South Africa. Fax: +27 21 938 9863.
E-mail address: celiavdm@sun.ac.za (C. van der Merwe).

http://dx.doi.org/10.1016/j.bbrc.2014.03.151
0006-291X/

[4]. *Parkin* encodes an E3 ubiquitin ligase protein, which forms part of the ubiquitin–proteasome system (UPS) whereby cytosolic, secretory and membrane proteins undergo degradation [5]. These unwanted proteins are tagged for removal by the parkin protein, which has also been involved in the removal of dysfunctional mitochondria from the cell via the process of mitophagy (selective degradation of mitochondria). Absence of parkin is thought to lead to the accumulation of critical substrates, resulting in the initiatory events that induce changes in mitochondrial structure and function [6].

Animal knockout models of *parkin* show several changes in the mitochondria in comparison to the wild-type controls. A study on a *Drosophila* knockout model revealed that mitochondrial defects were a common characteristic of the pathology [7]. Severe morphological features were observed, including irregular and dispersed myofibrillar arrangements and swollen and malformed mitochondria with disintegration of cristae. In mice knockout models, a decrease in the number of proteins involved in mitochondrial function and oxidative stress, lowered respiratory capacity of striated muscle mitochondria, as well as decreased serum antioxidant capacity were observed [8]. Human studies performed on leukocytes, fibroblasts and post mortem brain tissue obtained from PD patients with *parkin*-null mutations have further implicated structural and functional mitochondrial impairment [9–13]. In particular, human fibroblasts have been used as a primary cell model of PD [14], as expression levels of parkin are at relevant quantities in these cells.

Studies on fibroblasts have noted ultrastructural changes in the mitochondria such as larger mitochondrial mass [9] as well as grossly swollen mitochondria with disintegrated cristae [12]. However, studies on the mitochondrial network in fibroblasts have been controversial. Findings include no differences in the network of patient fibroblasts compared to controls [9], or an increase in mitochondrial branching in patient cells, indicating a possible increase in fusion [11]. Other studies have observed a fragmented mitochondrial network, suggesting that impaired mitochondrial fusion is present in *parkin*-null mutants [12].

Functional studies on the respiratory capacity of the mitochondrial electron transport chain complexes have shown a significant decrease in the activity of complex I in both fibroblasts and leukocytes from patients with *parkin* mutations in comparison to age-matched controls [15]. Impaired mitochondrial respiration usually results in ATP depletion which causes increased levels of reactive oxygen species (ROS), and eventually cell death. Studies on fibroblasts from *parkin*-null patients have shown varying results regarding the levels of ATP, with some showing significant reduction [9,11] and others showing a significant increase in ATP levels [12].

It is clear that further studies on fibroblasts harboring *parkin*-null mutations are needed, as previous studies have produced conflicting findings. In the present study, mitochondrial functional and structural analysis was performed on fibroblasts from three PD patients, all with *parkin*-null mutations. Muscle biopsies were assessed for mitochondrial defects. Furthermore, two heterozygous carriers of the *parkin*-null mutations were included for comparison with the homozygous patients.

2. Materials and methods

2.1. Ethics statement

The study protocol was approved by the Health Research Ethics Committee at Stellenbosch University, South Africa (Protocol number 2002/C059) and all study participants provided informed written consent.

2.2. Study participants

For the present study, three PD patients, each with two *parkin* null mutations were selected, one sporadic patient with Mixed Ancestry ethnicity (P1) and two White Afrikaner siblings (P2 and P3). The patients were examined by a movement disorder specialist (JC), and all met the UK Parkinson's Disease Society Brain Bank Research criteria for diagnosis of PD [16]. The exonic deletion mutations had been identified in these patients in previous studies using multiplex ligation-dependent probe amplification (MLPA) and cDNA sequencing; P1 has homozygous deletions of exons 3 and 4, whereas P2 and P3 have homozygous deletions of exon 4 [17–19]. Also included in the study were unaffected family members of the patients who are heterozygous carriers of the mutations. These included P1het (the mother of patient P1) and P2het (the sibling of sisters P2 and P3). In addition, two wild-type controls, WTC1 and WTC2, were included who did not harbor mutations in parkin and had no history of neurological disease. Phenotypic and genotypic data of the PD patients, heterozygous carriers and controls are summarized in Supplementary Table 1.

2.3. Fibroblast culture from skin biopsies

Fibroblasts were obtained from all three PD patients, both carriers and both WT controls, from a skin punch biopsy taken from the inner upper arm. The 2 mm × 2 mm skin piece was suspended in a solution of Dulbecco's Modified Eagle's Medium (DMEM; Lonza, Switzerland) with 10% fetal calf serum and 1% penicillin (1000 U/ml) streptomycin (1000 U/ml). The cells were grown in 25 cm^2 culture flasks at 37 °C, 5% CO_2. For all experiments the passage number was kept to below 12.

2.4. Muscle biopsies

Muscle biopsies were obtained from patients P1 and P2 but not from P3 as she exhibited severe tardive dyskinesias on the day of the procedure. Muscle biopsies were not requested from the WT controls or the carriers. For the biopsies an area of skin overlying the vastus lateralis muscle was sterilely prepared with 5% povidone iodine and 0.5% chlorhexidine. Thereafter, 2% lignocaine hydrochloride local anesthetic was injected intra- and subcutaneously in a 4 cm^2 area. A 1 cm longitudinal incision was made through the skin and fascia, and three percutaneous muscle biopsies were extracted using a 5 mm Bergström biopsy needle. A piece of muscle tissue was dissected with a scalpel and immediately fixed in gluteraldehyde buffer for electron microscopy studies. The remainder of the muscle tissue was snap frozen and stored in liquid nitrogen until sectioning.

2.5. Live cell imaging and analysis of mitochondrial morphology

Mitochondrial morphology was assessed by fluorescence microscopy. Human fibroblasts were seeded in Lab-Tek 8-well coverglasses (Nunc, 155411, Thermo Scientific). Mitochondria were stained with 200 nM Mitotracker Red (Invitrogen, Life Technologies, USA) and nuclei counterstained with Hoechst 33342 (Invitrogen, Life Technologies, USA). Image acquisition was performed on an Olympus IX-81 microscope coupled to an MT-20 Xenon-arc burner (Olympus Biosystems GMBH) and equipped with a F-view-II cooled CCD camera (Soft Imaging systems) and an environmental chamber (Solent Scientific). Images were acquired using 360 nm and 572 nm excitation and a UBG triple bandpass emission filter cube (Chroma). Z-stacking was performed with an increment of 0.26–0.3 μm between image frames, using an Olympus Plan Apo N60x/1.4 oil immersion objective. A total of 7–12 image frames

per stack were acquired, using the Cell^R software (Olympus) and exported as TIFF files for further processing and analysis.

The live cell imaging experiments were done in triplicate ($n = 3$) and a total of ten images were taken per sample for each experimental run. Clearly visible cells were individually analyzed using Image J 1.41o software giving a total average of 80 cells analyzed per sample across all experimental runs. All images were optimized by contrast adjustment and binarized by conversion to 8 bit image types. Unspecific noise of the fluorescent signal was reduced and a threshold applied to the images. Using Image J, morphological characteristics of each mitochondrion per cell were analyzed, including area, perimeter, as well as major and minor axes. These individual parameters were used to calculate mitochondrial mass, the aspect ratio (ratio between the major and minor axes of the ellipse equivalent to the object), and its form factor (perimeter^2/(4π × area)), which is consistent with the degree of branching.

2.6. Structural and ultrastructural analysis of the muscle biopsies and the fibroblasts

Transmission electron microscopy (TEM) was performed on both the muscle fibers and the fibroblasts to identify ultrastructural changes in the cells and mitochondria of patients and carriers in comparison to the wild type controls. Muscle biopsies were orientated and frozen in n-pentane, which was cooled in liquid nitrogen. 10–20 μm cryostat sections were cut. In addition to the section stained with hematoxylin and eosin, the following histochemical stains were performed routinely at 37 °C in a humidity chamber: Adenosine Triphosphatase (ATPase); Nicotinamide Adenine Dehydrogenase (NADH); Succinate Dehydrogenase (SDH). Furthermore, Periodic Acid Schiffs (PAS); Oil red O and Gomori Trichrome stains were performed. The sections for light microscopy were viewed using the Olympus BX41 microscope (Olympus, Germany).

The portion for electron microscopy was post-fixed in 1% osmium tetroxide, stained en-bloc with uranyl acetate and then dehydrated through graded alcohols and embedded in Epoxy resin. One micrometer thick sections were stained with 1% toluidine blue in 5% Borax. Six ultrathin sections were mounted on copper grids and stained with a saturated solution of uranyl acetate, followed by lead citrate for 6 min each. Ultrastructural investigation was performed using a Zeiss EM109 transmission electron microscope (Oberkochen, Germany).

The fibroblast cells were processed with a Leica automatic tissue processor. Sections were cut with glass knives, using Leica ultra-microtome, and placed on 200 mesh copper grids. The grids were scoped with a JEOL 10-11 transmission microscope (JEOL, Japan) and a SIS imaging system was used to view the cells.

2.7. Assessment of intracellular ATP levels

ATP levels were determined using the Enliten ATP Bioluminescence Detection kit (Promega, USA). The assay uses recombinant luciferase to catalyze the following reaction:

$$\text{ATP} + \text{D-Luciferin} + O_2 \rightarrow \text{Oxyluciferin} + \text{AMP} + \text{PPi} + CO_2 + \text{Light}$$

The intensity of the emitted light is proportional to the ATP concentration.

Fibroblasts were seeded in 25 cm^2 flasks at a count of 100,000 cells per individual and incubated at 37 °C, 5% CO_2 until they reached 80% confluence. Following this, the fibroblasts were trypsinized and collected by centrifugation at 1000 rpm and washed with PBS. The cell pellets were resuspended in 50 μl ice cold extraction buffer (100 mM Tris–HCl and 4 mM EDTA, pH 7.75). Immediately thereafter, 150 μl boiling extraction buffer was added and samples were incubated at 99 °C for 2 min. Thereafter, the samples were centrifuged at 10 000 rpm for 1 min and supernatants were collected. Measurement of ATP levels was performed in three separate experiments ($n = 3$), each in duplicate on a luminometer, using 50 μl sample and 50 μl of luciferase reagent.

2.8. Statistical analysis

Linear mixed-effects models of the various outcomes mitochondrial mass, aspect ratio, form factor and ATP levels, were used with predictors individuals and groups (patients, heterozygote carriers and WT controls), respectively, as fixed effects. Experiments, individuals (when comparing groups) and an indicator of relatedness were used as random effects, to adjust the correlation between individuals and between experiments inside individuals and for relatedness (grouping of family members). The values for both mitochondrial mass and ATP levels and were log transformed to approximate normality prior to analysis. The freely available program R (www.r-project.org) and function lme from the R package nlme was used for the analysis [20]. p values of <0.05 were regarded as statistically significant.

3. Results

3.1. Mitochondrial network was unaffected

Given that the functional state of mitochondria is often reflected in their morphology, we investigated various morphological parameters such as form factor, aspect ratio and mitochondrial mass in all patients and carriers compared to control cells. For all parameters no differences were observed either at an individual level or as groups ($p > 0.05$ for all) (Fig. 1A and B).

3.2. Ultrastructural alterations observed

TEM was used for more detailed ultrastructural analysis of the mitochondrial morphology. The fibroblasts of the control (Fig. 2A) showed rod-like shaped mitochondria, with intact cristae and membranes. Vacuoles present in the control cells were predominantly clear. By comparison, electron-dense (darker) vacuoles thought to be lysosomes were observed in all three patients, but to a lesser degree in P3 (Fig. 2B–D). In addition, mostly spherical mitochondria were observed in patient P1's fibroblasts (Fig. 2B). Fig. 2E indicates a mitochondrion possibly in the process of being engulfed by autophagosomal or lysosomal structures, and thus it could be speculated that the electron dense material is degraded mitochondria. No ultrastructural alterations were evident in the heterozygous carriers (data not shown).

3.3. Decreased ATP levels

Two of the patients exhibited statistically significant lower ATP levels compared to an average of the controls. Patients P1 and P2 showed a 41.8% ($p = 0.0091$) and 36.3% ($p = 0.0195$) decrease, respectively (Fig. 3). Patient P3 showed only a 9.3% decrease, which was not statistically significant ($p = 0.5022$). Although both carriers showed no statistically significant difference in ATP levels, P2het exhibited a 29.4% decrease ($p = 0.0893$).

In addition, the three groups i.e. patients, carriers and controls were simultaneously compared, yielding a combined p-value of 0.0191. Investigating pairwise differences, the combined patients differed highly significantly from the controls (29% decrease, $p = 0.0058$), whereas the carriers did not differ significantly from the controls (15% decrease, $p = 0.1584$).

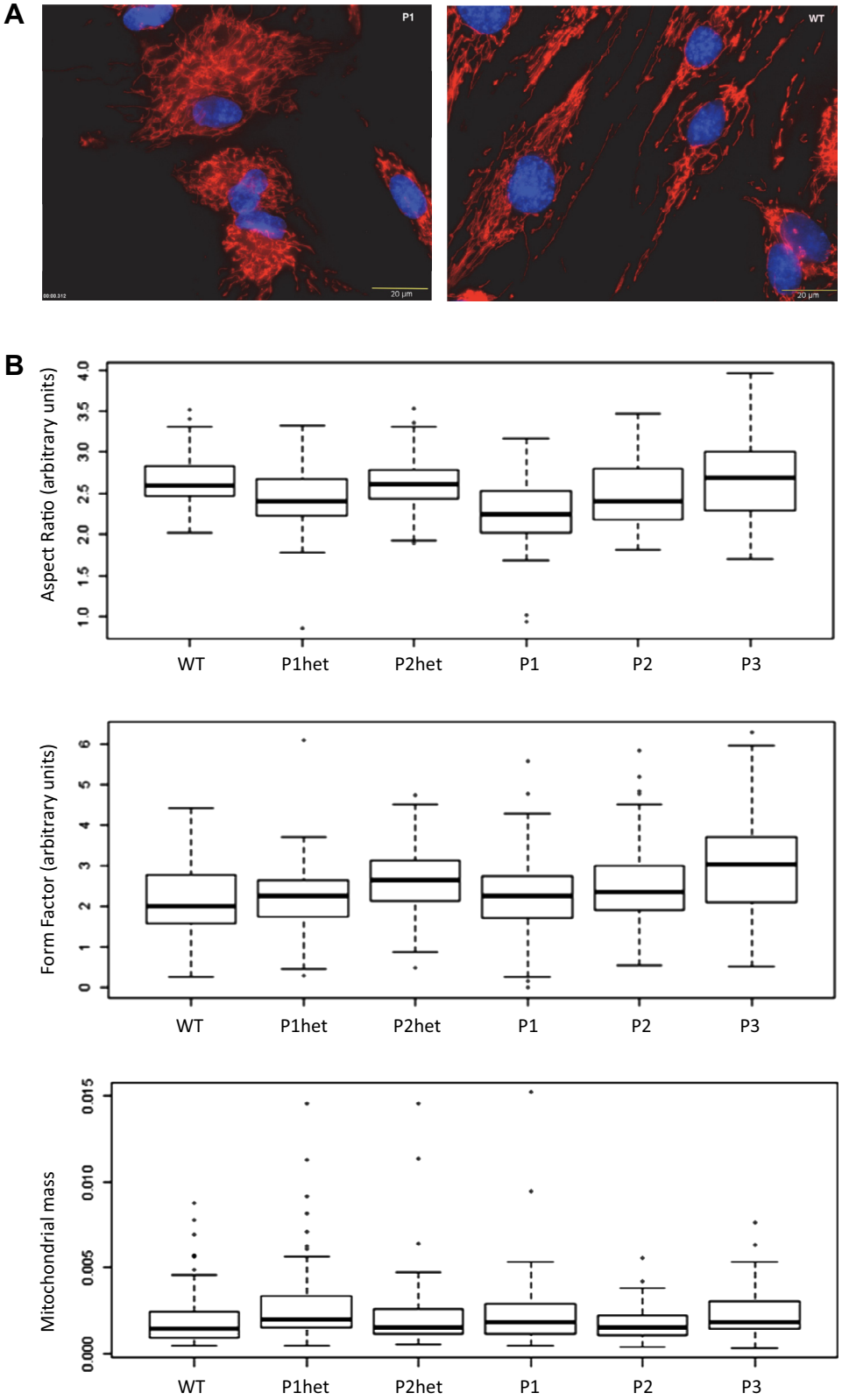

Fig. 1. Morphology of the mitochondrial network in fibroblasts. (A) Representative images of control and parkin-mutant fibroblasts. Mitotracker Red was used to visualize the mitochondrial network and the nuclei were counterstained with Hoechst 33342. Scale bar: 20 µm. (B) Boxplots showing the distributions of aspect ratio, form factor and mitochondrial mass, and analysis of the data revealed that there were no differences in mitochondrial branching between the patient, carrier and control groups ($p > 0.05$).

3.4. Subtle abnormalities detected in muscle

No significant abnormalities were found on light microscopic examination of the muscle biopsy of P1 whereas for P2 a mild degree of muscle fiber atrophy was found, which was regarded as non-significant and probably age related. Except for focal accumulations of slightly swollen mitochondria, no mitochondrial abnormalities were detected on TEM of either muscle biopsy

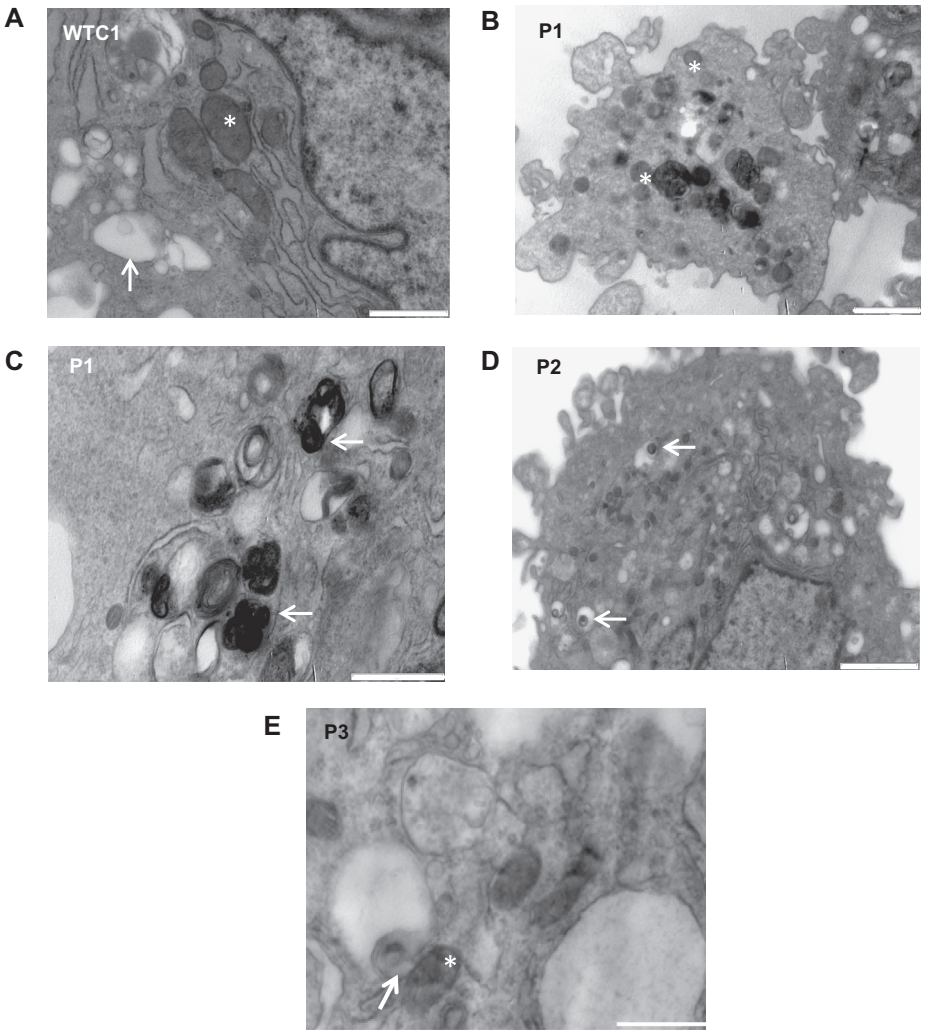

Fig. 2. Transmission electron microscopy images of fibroblasts. (A) Fibroblasts of the control indicating rod-like shaped mitochondria (asterix), and clear vacuoles (arrow). (B) Spherical mitochondria (asterix) and (C) dark, electron-dense vacuoles (arrow) were observed in patient P1 and (D) P2's cells. (E) In patient P3's fibroblasts the presence of a mitochondrion (asterix) close to a vacuole (arrow) is observed, which may be an indication that the mitochondrion is in the process of being engulfed. Scale bar: A and C, 1 μm; B and D, 2 μm; E, 0.5 μm.

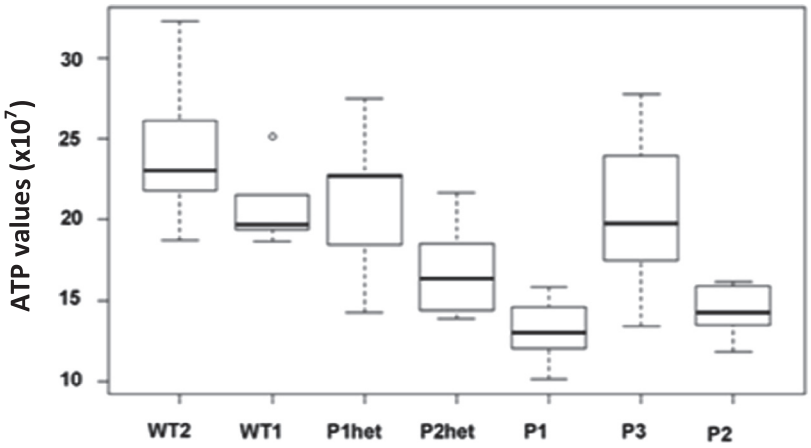

Fig. 3. Boxplots showing distributions of ATP levels. ATP levels were measured in arbitrary units of ATP luminescence and significant differences were found between the patient and control groups.

(Fig. 4). Some folding of the sarcolemma was seen on TEM of both biopsies, a non-specific finding possibly related to mild atrophy. Additionally, accumulations of intermyofibrillar glycogen was visible on TEM of P2, the significance of which is uncertain.

4. Discussion

In the present study, we investigated the effect of *parkin*-null mutations on the structure and function of mitochondria in fibro-

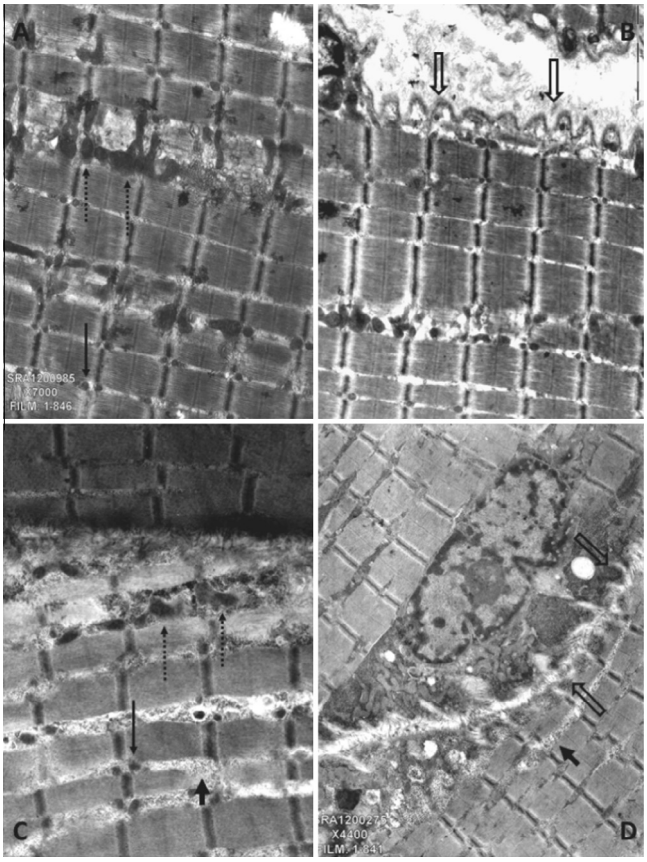

Fig. 4. Transmission electron microscopy images of muscle fibers. (A and B) Patients P1 and (C and D) P2. Normal appearing mitochondria (solid, thin arrows) and slightly swollen mitochondria (dashed arrows) can be seen in the muscle of both patients (images A and C). Folding of the sarcolemma, probably indicative of mild atrophy can also be seen in both biopsies (open arrows; images B and D). Additionally, small collections of intermyofibrillar glycogen can be seen in the images from P2 (short arrows, images C and D).

blasts obtained from South African PD patients. Although no differences were observed in the mitochondrial network, subtle morphological alterations and decreased ATP levels were found in two of the three patients compared to the controls. No defects were observed in the heterozygous mutation carriers. In muscle biopsies obtained from two of the patients subtle abnormalities were detected.

Structural analysis of the mitochondrion allows identification of defects which could impair mitochondrial function, and that could ultimately affect the overall cellular function. Tubular networks are formed through the processes of fusion and fission, and provide an indication of the maintenance of mitochondrial function. In the present study we found no differences in the mitochondrial network morphology between the patients and the controls. This concurs with a previous study on parkin-mutant fibroblasts that also showed no differences under basal culturing conditions [9]. It has been speculated that parkin- and PINK1-deficient cells may require additional stressors (rotenone, paraquat, oxidative stress, etc.) to induce a mitochondrial fragmentation phenotype [9,21,22].

Ultrastructural analysis of the patients' fibroblasts revealed a mixture of rod-shaped and circular mitochondria that appeared swollen, as well as electron dense autophagic vacuoles, which has been observed previously [12]. Cellular vacuoles house hydrolytic enzymes (lysosomes), and function as exporters of waste in the cell. The cellular material observed within these vacuoles may be accumulated proteins or damaged mitochondria which are aggregating due to the absence of parkin, thus resulting in autophagosomes. However, further work is needed to determine the nature of the material inside these vacuoles before any conclusions can be drawn.

In addition, significantly decreased ATP levels were detected in two of the three patients. This corresponds with the hypothesis that ATP generation in these fibroblasts is predominantly via the less efficient glycolysis pathway. Previous studies have conflicted with regards to ATP levels, although some of these seem to agree that ATP levels are decreased in patient fibroblasts with *parkin* mutations [9,11].

The significance of the muscle fiber atrophy observed on TEM of both patients is uncertain, as it was very mild and is a non-specific finding. In the case of P2, where it was also seen on light microscopy, this finding can probably be explained by sarcopenia (the loss of skeletal muscle mass and strength as a result of aging) as P2 is 13 years older than P1. Although it would be expected that more severe mitochondrial alterations would be reflected in the more energy-demanding muscle tissue, the changes detected in the fibroblasts were not observed in the muscle fibers. The reasons for this discrepancy are not known but generally, post-mitotic tissue with high metabolic energy requirements, such as muscle, is preferentially affected in mitochondrial disorders. However, these disorders, caused by either mitochondrial or DNA mutations, directly affect energy production. Whether the same holds true for mutations that are implicated in altered mitophagy or ubiquitination of substrate proteins, as seen in *parkin* mutations, is unknown. Of note, mutations in *MFN2*, which encodes the mitochondrial-fusion promoting factor mitofusin 2, and cause an inherited neuropathy are not known to affect muscle tissue [23]. To our knowledge there has only been one other published report on muscle morphology in a parkin-mutant patient [24]. This study found features of mitochondrial muscle pathology in a single patient but whether the two conditions, PD and mitochondrial myopathy were unrelated and occurred co-incidentally in this patient is not clear. The pattern of mitochondrial involvement in PD and related disorders therefore remains to be investigated.

A limitation of the present study was the limited number of samples and therefore follow-up studies will include larger numbers of patients and controls. Future studies will also focus on measuring ATP synthesis rates, the activity of individual mitochondrial complexes, ROS levels and the mitochondrial membrane potential. Moreover, although fibroblasts have been shown to be a good cell model to study disease mechanisms in PD [14], it would be of interest to determine whether the defects that we have observed, and other features of oxidative stress [25], are also present in neural cells generated from induced pluripotent stem cells (iPSCs) of these and other PD patients.

In conclusion, our results on South African patients concur with previous studies that mitochondrial dysfunction is present in PD patients with *parkin* null mutations. Subtle alterations were found in the mitochondria of the fibroblasts at both a morphological and functional level. Interestingly, one of the three patients (P3) did not show these defects. The reasons for this are currently unknown although the patient is known to have had a less severe phenotype and a slower disease progression in comparison to her sibling (P2). These preliminary findings indicate that there may be compensatory biological mechanisms such as differences in autophagic activity which could result in different phenotypes being observed between individuals when using patient-derived cells. These compensatory mechanisms may in part explain the variable and conflicting results reported to date. Further work is necessary in iPSC-derived neurons from larger numbers of patients harboring PD-causing mutations and controls in order to determine if the observed differences found in fibroblasts are mirrored in neuronal cells.

Acknowledgments

We would like to acknowledge the patients, their families and the controls for their participation in this study, and Sr. Debbie Lombard for patient recruitment.

Appendix A. Supplementary data

Supplementary data associated with this article can be found, in the online version, at http://dx.doi.org/10.1016/j.bbrc.2014.03.151.

References

[1] L.M.L. de Lau, M.M.B. Breteler, Epidemiology of Parkinson's disease, Lancet Neurol. 5 (2006) 525–535, http://dx.doi.org/10.1016/S1474-4422(06)70471-9.
[2] T. Gasser, Mendelian forms of Parkinson's disease, Biochim. Biophys. Acta 1792 (2009) 587–596, http://dx.doi.org/10.1016/j.bbadis.2008.12.007.
[3] S. Lubbe, H.R. Morris, Recent advances in Parkinson's disease genetics, J. Neurol. (2013), http://dx.doi.org/10.1007/s00415-013-7003-2.
[4] T. Kitada, S. Asakawa, N. Hattori, H. Matsumine, Y. Yamamura, S. Minoshima, et al., Mutations in the parkin gene cause autosomal recessive juvenile parkinsonism, Nature 392 (1998) 605–608, http://dx.doi.org/10.1038/33416.
[5] T.M. Dawson, Molecular pathways of neurodegeneration in Parkinson's disease, Science 302 (2003) 819–822, http://dx.doi.org/10.1126/science.1087753.
[6] P.J. Kahle, C. Haass, How does parkin ligate ubiquitin to Parkinson's disease?, EMBO Rep 5 (2004) 681–685, http://dx.doi.org/10.1038/sj.embor.7400188.
[7] J.C. Greene, A.J. Whitworth, I. Kuo, L.A. Andrews, M.B. Feany, L.J. Pallanck, Mitochondrial pathology and apoptotic muscle degeneration in Drosophila parkin mutants, Proc. Natl. Acad. Sci. U. S. A. 100 (2003) 4078–4083, http://dx.doi.org/10.1073/pnas.0737556100.
[8] J.J. Palacino, Mitochondrial dysfunction and oxidative damage in parkin-deficient mice, J. Biol. Chem. 279 (2004) 18614–18622, http://dx.doi.org/10.1074/jbc.M401135200.
[9] A. Grünewald, L. Voges, A. Rakovic, M. Kasten, H. Vandebona, C. Hemmelmann, et al., Mutant parkin impairs mitochondrial function and morphology in human fibroblasts, PLoS One 5 (2010) e12962, http://dx.doi.org/10.1371/journal.pone.0012962.
[10] H.-H. Hoepken, S. Gispert, B. Morales, O. Wingerter, D. Del Turco, A. Mülsch, et al., Mitochondrial dysfunction, peroxidation damage and changes in glutathione metabolism in PARK6, Neurobiol. Dis. 25 (2007) 401–411, http://dx.doi.org/10.1016/j.nbd.2006.10.007.
[11] H. Mortiboys, K.J. Thomas, W.J.H. Koopman, S. Klaffke, P. Abou-Sleiman, S. Olpin, et al., Mitochondrial function and morphology are impaired in parkin-mutant fibroblasts, Ann. Neurol. 64 (2008) 555–565, http://dx.doi.org/10.1002/ana.21492.
[12] C. Pacelli, D. De Rasmo, A. Signorile, I. Grattagliano, G. di Tullio, A. D'Orazio, et al., Mitochondrial defect and PGC-1α dysfunction in parkin-associated familial Parkinson's disease, Biochim. Biophys. Acta 2011 (1812) 1041–1053, http://dx.doi.org/10.1016/j.bbadis.2010.12.022.
[13] F.R. Wiedemann, K. Winkler, H. Lins, C.-W. Wallesch, W.S. Kunz, Detection of respiratory chain defects in cultivated skin fibroblasts and skeletal muscle of patients with Parkinson's disease, Ann. N. Y. Acad. Sci. 893 (1999) 426–429, http://dx.doi.org/10.1111/j.1749-6632.1999.tb07870.x.
[14] G. Auburger, M. Klinkenberg, J. Drost, K. Marcus, B. Morales-Gordo, W.S. Kunz, et al., Primary skin fibroblasts as a model of Parkinson's disease, Mol. Neurobiol. 46 (2012) 20–27, http://dx.doi.org/10.1007/s12035-012-8245-1.
[15] M. Müftüoglu, B. Elibol, O. Dalmizrak, A. Ercan, G. Kulaksiz, H. Ogüs, et al., Mitochondrial complex I and IV activities in leukocytes from patients with parkin mutations, Mov. Disord. Off. J. Mov. Disord. Soc. 19 (2004) 544–548, http://dx.doi.org/10.1002/mds.10695.
[16] W.R. Gibb, A.J. Lees, The relevance of the Lewy body to the pathogenesis of idiopathic Parkinson's disease, J. Neurol. Neurosurg. Psychiatry 51 (1988) 745–752, http://dx.doi.org/10.1136/jnnp.51.6.745.
[17] S. Bardien, R. Keyser, Y. Yako, D. Lombard, J. Carr, Molecular analysis of the parkin gene in South African patients diagnosed with Parkinson's disease, Parkinsonism Relat. Disord. 15 (2009) 116–121, http://dx.doi.org/10.1016/j.parkreldis.2008.04.005.
[18] W.L. Haylett, R.J. Keyser, M.C. du Plessis, C. van der Merwe, J. Blanckenberg, D. Lombard, et al., Mutations in the parkin gene are a minor cause of Parkinson's disease in the South African population, Parkinsonism Relat. Disord. 18 (2012) 89–92, http://dx.doi.org/10.1016/j.parkreldis.2011.09.022.
[19] R.J. Keyser, D. Lombard, R. Veikondis, J. Carr, S. Bardien, Analysis of exon dosage using MLPA in South African Parkinson's disease patients, Neurogenetics 11 (2010) 305–312, http://dx.doi.org/10.1007/s10048-009-0229-6.
[20] J.P. (S version), D.B. (up to 2007), S.D. (up to 2002), D.S. (up to 2005), E. authors, R-core, nlme: Linear and Nonlinear Mixed Effects Models, 2013.
[21] A. Sandebring, N. Dehvari, M. Perez-Manso, K.J. Thomas, E. Karpilovski, M.R. Cookson, et al., Parkin deficiency disrupts calcium homeostasis by modulating phospholipase C signalling, FEBS J. 276 (2009) 5041–5052, http://dx.doi.org/10.1111/j.1742-4658.2009.07201.x.
[22] A. Grünewald, M.E. Gegg, J.-W. Taanman, R.H. King, N. Kock, C. Klein, et al., Differential effects of PINK1 nonsense and missense mutations on mitochondrial function and morphology, Exp. Neurol. 219 (2009) 266–273, http://dx.doi.org/10.1016/j.expneurol.2009.05.027.
[23] K. Verhoeven, K.G. Claeys, S. Züchner, J.M. Schröder, J. Weis, C. Ceuterick, et al., MFN2 mutation distribution and genotype/phenotype correlation in Charcot–Marie–Tooth type 2, Brain J. Neurol. 129 (2006) 2093–2102, http://dx.doi.org/10.1093/brain/awl126.
[24] H.A. Hanagasi, P. Serdaroglu, M. Ozansoy, N. Basak, H. Tasli, M. Emre, Mitochondrial pathology in muscle of a patient with a novel parkin mutation, Int. J. Neurosci. 119 (2009) 1572–1583.
[25] Y. Imaizumi, Y. Okada, W. Akamatsu, M. Koike, N. Kuzumaki, H. Hayakawa, et al., Mitochondrial dysfunction associated with increased oxidative stress and α-synuclein accumulation in PARK2 iPSC-derived neurons and postmortem brain tissue, Mol. Brain 5 (2012) 35, http://dx.doi.org/10.1186/1756-6606-5-35.